Climate Dynamics
https://doi.org/10.1007/s00382-022-06160-0

Long-term trends in the Southern Annular Mode from transient Mid- to Late Holocene simulation with the IPSL-CM5A2 climate model

Gabriel Silvestri[1] · **Ana Laura Berman**[1] · **Pascale Braconnot**[2] · **Olivier Marti**[2]

Received: 28 August 2021 / Accepted: 18 January 2022

Abstract
This study describes time evolution of the Southern Annular Mode (SAM) in Mid- to Late Holocene simulated with a state-of-the-art transient simulation of the last 6000 years carried out with the IPSL-CM5A2 model. Simulated SAM index exhibits significant long-term linear trends of different sign depending on the season that are closely related to multi-millennial changes in insolation which was the main driver of long-term climate change in the study period. Interactions between changes in insolation and the SAM are linked to temperature and pressure changes developed through the entire Southern Hemisphere. In fact, model results suggest that insolation changes produced significant changes in extratropical temperature gradients that, in turn, induced changes in pressure gradients synthesized by significant long-term linear trends in the SAM index from Mid- to Late-Holocene. Considering that changes in the SAM index synthetize changes in hemispheric patterns of temperature, pressure and winds, results exposed in this study should be considered as reference for reconstructions of SAM evolution in the last 6000 years from climate proxy archives.

Keywords Southern Annular Mode · IPSL-CM5A2 model · Holocene · Southern Hemisphere

1 Introduction

The Southern Annular Mode (SAM), also referred as High Latitude Mode or Antarctic Oscillation in pioneer papers, is the leading Empirical Orthogonal Function of Southern Hemisphere atmospheric circulation variability at extratropical latitudes (e.g., Rogers and van Loon 1982; Kidson 1988, 1999; Limpasuvan and Hartmann 2000; Thompson and Wallace 2000). The spatial structure of the SAM is almost similar year-round being characterized by strong zonal symmetry with synchronous anomalies of opposite sign over middle and high latitudes through the entire troposphere on daily to decadal times scales (e.g., Kidson 1999; Mo 2000; Baldwin 2001; Cai and Watterson 2002; Fogt and Bromwich 2006). The corresponding Principal Component time series is usually referred as the SAM index. The positive SAM phase (i.e., positive value in the SAM index) is defined by anomalously high pressure in middle latitudes (~40° S) relative to anomalously low pressures over Antarctica (~65° S) while inverse pressure anomalies relation defines the negative SAM phase (i.e., negative value in the SAM index).

Conceptually, the SAM synthesizes the seesaw pattern (negative correlation) that exists between pressure anomalies at middle and high latitudes in the Southern Hemisphere. This pattern of atmospheric circulation anomalies is closely related to changes in position and intensity of the southern westerlies that encircle mid-high latitudes (~50° S to ~70° S): the westerlies tend to intensify and the latitude of maximum wind speed shifts toward Antarctica when the SAM index increases while the westerlies tend to weaken and the maximum wind moves toward the equator when the SAM index decreases (see more details in

✉ Gabriel Silvestri
gabriels@cima.fcen.uba.ar

Ana Laura Berman
alberman@cima.fcen.uba.ar

Pascale Braconnot
pascale.braconnot@lsce.ipsl.fr

Olivier Marti
olivier.marti@lsce.ipsl.fr

[1] Universidad de Buenos Aires (UBA)-CONICET-Instituto Franco-Argentino para el Estudio del Clima y sus Impactos (IRL 3351 IFAECI)/CNRS-IRD-CONICET-UBA, Buenos Aires, Argentina

[2] Laboratoire des Sciences du Climat et de l'Environnement, LSCE/IPSL, CEA-CNRS-UVSQ, Université Paris-Saclay, Gif-sur-Yvette, France

Published online: 31 January 2022

Sect. 3). Additionally, several studies demonstrated significant influence of the SAM on surface weather and climate variability at middle and high latitudes of the Southern Hemisphere (e.g., Fogt and Marshall 2020, and references therein). Although the SAM is consequence of internal atmospheric dynamical processes (e.g., Limpasuvan and Hartmann 2000), its intensity and phase can be markedly affected by external forcings such as changes in greenhouse gas and stratospheric ozone concentrations (e.g., Thompson and Solomon 2002; Cai et al. 2003; Shindell and Schmidt 2004; Arblaster and Meehl 2006; Miller et al. 2006; Polvani et al. 2011; Fogt et al. 2017) and changes in solar irradiance (e.g., Kuroda and Kodera 2005; Kuroda and Shibata 2006). A complete review of key aspects of the scientific literature regarding SAM variability, climate impacts, trends, and forcing was recently summarized by Fogt and Marshall (2020).

Atmospheric reanalyses allow detailed descriptions of SAM evolution and variability since 1979 when information from satellites is available. For previous periods, the lack of meteorological information over wide portions of the Southern Hemisphere reduces the quality of those gridded data sets. However, Marshall (2003) provided a reconstruction of the SAM index since 1957 based on information from meteorological stations located at ~ 40° S and ~ 65° S. Additionally, Fogt et al. (2009) and Visbeck (2009) reconstructed the SAM index to the last decades of the nineteenth century allowing studies of SAM behavior over the past ~ 150 years. To extend the SAM record further back, a wide variety of climate proxy data and methodologies were employed. In fact, Jones and Widmann (2003), Zhang et al. (2010), Villalba et al. (2012), Abram et al. (2014), and Dätwyler et al. (2018) reconstructed time evolution of the SAM index through past centuries. In particular, Abram's and Dätwyler's reconstructions cover the entire past millennium suggesting that the pronounced positive trend in the SAM index observed recently and attributed to the action of anthropogenic climate forcing (e.g., Sexton 2001; Thompson and Solomon 2002; Gillett and Thompson 2003; Arblaster and Meehl 2006; Thompson et al. 2011) is unprecedented over past centuries. Although there are some inconsistencies among reconstructed indices, especially before the nineteenth century (Hessl et al. 2017; Hernández et al. 2020), all of them agree in a pronounced positive trend since the ~ 1950s. Differences among reconstructed SAM index prior to the window over which the proxies are calibrated might be consequence of non-stationary proxy-SAM teleconnections (Huiskamp and McGregor 2020).

Reconstructions mentioned in the previous paragraph demonstrate the significant effort made to reconstruct long records of SAM variability. However, there is still a lack of proxy-based reconstructions of the SAM extended more than the past millennium. Although this information is essential to assess long-term trends prior to the influence of modern anthropogenic forcing, the lack of appropriated climate proxy records makes difficult to infer characteristics of the SAM before ~ 1000 years BP. In this context, the close relationship between SAM and position/intensity of southern westerlies suggests that reconstructed characteristics of these winds might be an alternative way to infer relevant features of past long-term SAM evolution. Unfortunately, there is not a clear consensus related to the evolution of the westerlies through the Holocene having marked discrepancies among available reconstructions regarding periods in which these winds reinforced/weakened or shifted southward/northward (Hernández et al. 2020; Laprida et al. 2021 and references therein). In light of these limitations in the available proxy information, numerical climate model simulations emerge as a valuable tool to infer how the SAM could have responded to long-term changes in natural climate forcings through the Holocene prior to the beginning of the modern Industrial Era in ~ 1850s. Additionally, numerical simulations can help to define the most relevant features of atmospheric circulation that should be the focus of future proxy-based studies related to reconstructions of past SAM behavior. In this context, the state-of-the-art multi-millennial transient simulations of global climate conditions from Mid- to Late Holocene carried out with the IPSL-CM5A2 model contain a continuous description of atmospheric variability during the last 6000 years. Consequently, these simulations provide an excellent opportunity to infer patterns of SAM evolution through that period. Therefore, the aim of our analysis is to investigate long-term changes in the SAM variability using the transient IPSL-CM5A2 model simulations. To the best of our knowledge, this study first describes SAM evolution considering a transient model simulation of the last 6000 years. This information is essential in order to have a complete picture of past climate evolution giving a long-term historical context of both present-day conditions and projected future changes. Additionally, results of this analysis might be a significant contribution to improve paleoclimatic studies focused on reconstructions of large-scale atmospheric circulation patterns in the Southern Hemisphere.

The article is organized as follows. Model simulation and methodology are described in Sect. 2. Modeled SAM index evolution in the study period is showed in Sect. 3. Available information from proxy-based reconstructions is discussed in Sect. 4. The influence of Pacific Ocean sea surface temperature (SST) on SAM evolution is analyzed in Sect. 5. The main conclusions are summarized in Sect. 6.

2 Model simulation and methodology

2.1 Model simulation

The present study uses IPSL-CM5A2, the Earth system model developed at IPSL (Institut Pierre Simon Laplace,

France). It couples atmosphere, land surface, ocean and sea-ice, and accounts for energy, water and carbon cycles. A complete description of the different components of this model version, the coupling scheme and model performances can be found in Dufresne et al. (2013), Mignot and Bony (2013), and Sepulchre et al. (2020). IPSL-CM5A2 is an enhancement of IPSL-CM5A, whose ability to reproduce the mid-Holocene climate (6000 years BP) was discussed in Kageyama et al. (2013a, b). This model represents all scale of variability from hours to centuries or millennium. For instance, Braconnot et al. (2019) used the transient climate simulation to characterize the multiscale variability of the Indian and West African monsoons in the last 6000 years concluding that the 2- to 20-year variability of the Holocene simulation changes in time with a good correlation to the orbital forcing, and the long-term trend is driven by the orbital forcing with a very strong correlation. Furthermore, Crétat et al. (2020) studied the model variability for the Indian monsoon region showing a large variability in the 50–500 year range in addition to the more traditional decadal variability.

The initial climate state in the multi-millennial IPSL-CM5A2 transient simulation corresponds to a Paleoclimate Modeling Intercomparison Project simulation run with 6000 years BP boundary conditions (Kageyama et al. 2018; Braconnot et al. 2019). After that, Earth's orbital parameters and atmospheric composition were updated each year from 6000 years BP to the present but the transient simulation does not include volcanic forcing (see more details in Braconnot et al. 2019). During the study period, the main driver of long-term climate change was the slow change in incoming solar radiation (insolation) at the top of the atmosphere due to changes in orbital parameters of the Earth around the Sun. Insolation mean values and changes over the Southern Hemisphere considering information contained in the IPSL-CM5A2 simulation are shown in Fig. 1 and Supplementary Fig. S1. The annual cycles show maximum (minimum) insolation in summer (winter) and reduction of values with increasing latitude including winter polar nights (Fig. 1a). Slow long-term changes from 6000 years BP to the present were characterized by increment of insolation from summer to autumn and reduced insolation from winter to spring (Fig. 1b). However, intensities and timing of these changes were not uniform through all latitudes of the Southern Hemisphere (Supplementary Fig. S1a) and the insolation forcing was almost constant through the last millennium (Supplementary Fig. S1b).

2.2 Methodology

Although the SAM is defined as the leading Empirical Orthogonal Function of extratropical Southern Hemisphere atmospheric variability, the SAM index analyzed in this study is calculated following the alternative methodology proposed by Gong and Wang (1999). Consequently, the SAM index (i.e., the time series equivalent to the first Principal Component time series) is calculated as the normalized difference between 40° S and 65° S in sea level pressure (SLP): $SAM_{INDEX} = SLP^{*}_{40°S} - SLP^{*}_{65°S}$ where $SLP^{*}_{40°S}$ and $SLP^{*}_{65°S}$ are normalized zonally mean SLP of 40° S and 65° S for every month respectively. The spatial field of the SAM (i.e., the spatial field equivalent to the first Principal Component spatial field) is calculated as the correlation of the SAM index with SLP anomalies in each grid point. An example of the use of this alternative methodology to calculate the SAM is displayed in Fig. 2 demonstrating the similarity with that based on Principal Component analysis in both spatial field and time series. Furthermore, this alternative methodology helps to expose that the SAM index synthesizes the strength of the meridional gradient of pressure anomalies at middle and high Southern Hemisphere latitudes.

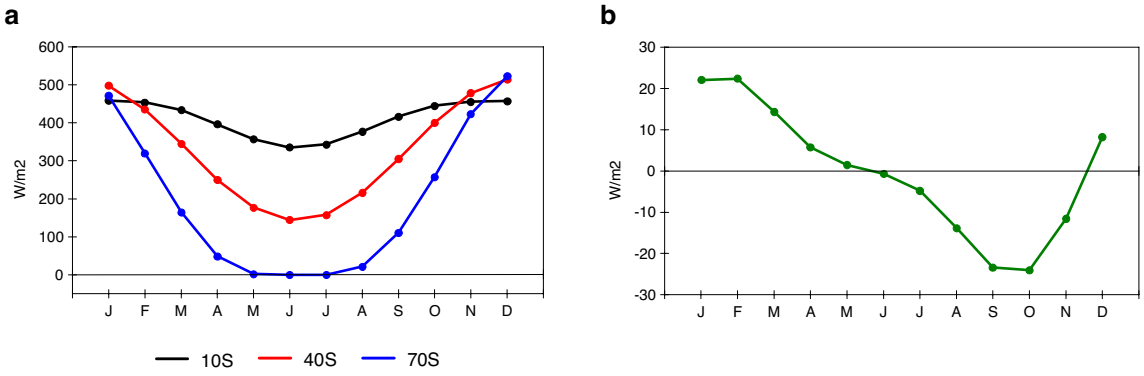

Fig. 1 **a** Annual cycle of present-day incoming solar radiation (insolation) at the top of the atmosphere averaged over 10° S, 40° S and 70° S in the IPSL-CM5A2 simulation. **b** Insolation changes in the band between 10° S and 70° S calculated as insolation in the present minus insolation in 6000 years BP

Simulations performed with the IPSL-CM5A2 model extend from 6000 years BP to the present considering the present (or year zero) to 1950. However, to exclude the incipient anthropogenic effect on climate system, the last simulated century (i.e., the period 1850–1950) is omitted in the analysis. Mean values and standard deviations involved in definition of the SAM index correspond to the period of 5900 years extended from 6000 years BP to 1849. The selection of this time period of reference does not affect the characteristics of SAM long-term trends showed through the study because those characteristics are independent of the precise time period over which zonally mean SLP is normalized.

In order to simplify descriptions of climate evolution through the Holocene, two specific time-periods are taken into account: the period identified as Mid-Holocene (MidH) corresponding to the initial period 6000–5500 years BP (i.e., the first five simulated centuries) and the period identified as Late Holocene (LatH) corresponding to the final period 1350–1849 (i.e., the last five simulated centuries previous to the beginning of the Industrial Era).

The study is based on modeled monthly mean values of sea level pressure (SLP), temperature at 2 m (T2m), and zonal component of wind at 850 hPa (U850). The statistical significance of linear trends is assessed considering the Student's *t* test (Wilks 2006).

3 Modeled evolution of the SAM index

Long-term evolution of the SAM index in Mid- to Late Holocene is displayed by changes of sign, monthly linear trends and time series on the whole period extended from 6000 years BP to 1849 (Fig. 3). Monthly evolutions reveal the occurrence of changes of sign and significant long-term linear trends with a clear annual pattern (Fig. 3a, b): significant positive trends from February to July and significant negative trends from September to December while January and August are months of transition in which linear trends are not statistically significant. This inverse behavior is summarized by the SAM index in austral autumn (March–April–May, MAM) and spring (September–October–November, SON) (Fig. 3c). Linear trends in monthly SAM index produced long-term shifts in the SAM phase (from negative to positive or vice versa depending on the month) which sign is related to the time-window taken as reference to calculate the corresponding anomalies (see Sect. 2.2). In this evolution, time series of modeled SAM (Fig. 3c) show a lack of trends during the last ~ 1500 years (see more details in Sect. 4).

As was mentioned in Sect. 1, the SAM index synthesizes the strength of the meridional gradient of pressure anomalies at middle and high Southern Hemisphere latitudes. Therefore, monthly linear trends displayed in Fig. 3 are consequence of long-term changes in pressure gradients through the study period. Actually, the extratropical meridional gradient of SLP (i.e., differences between zonal mean SLP at 40° S and 65° S) increased from February to August and decreased from September to January (Fig. 4a, b). These

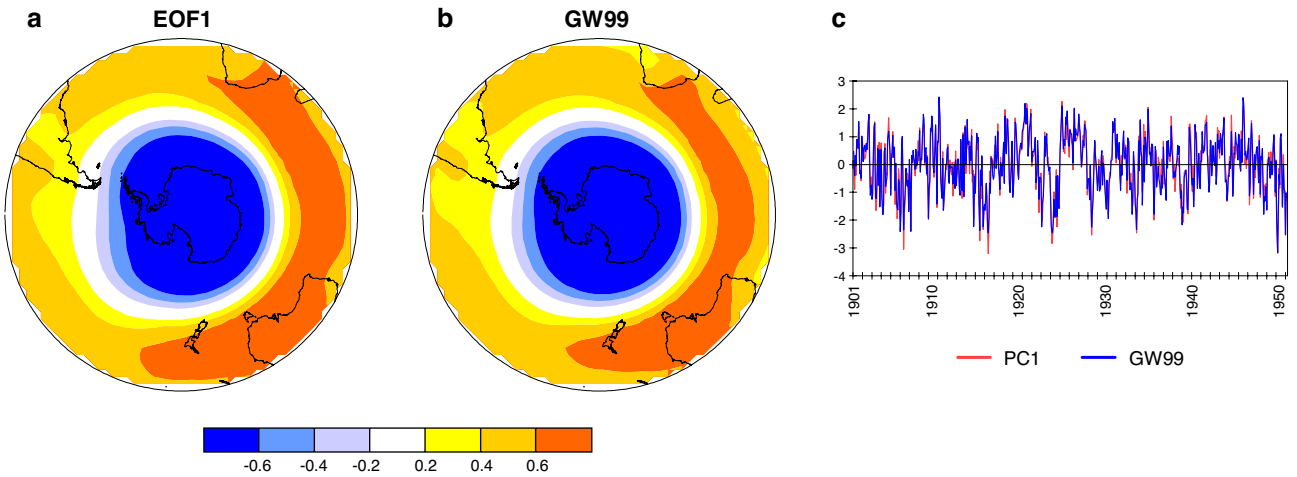

Fig. 2 **a** Leading empirical orthogonal function of monthly mean sea level pressure (SLP) poleward of 20° S simulated by the IPSL-CM5A2 model in 1901–1950. **b** Correlation map of the annual SAM index calculated as in Gong and Wang (1999) (GW99) using the time-varying SLP anomalies simulated by the IPSL-CM5A2 model in 1901–1950. **c** PC time series corresponding to **a** (red) and the SAM index used in **b** (blue). Correlation between these time series is 0.98

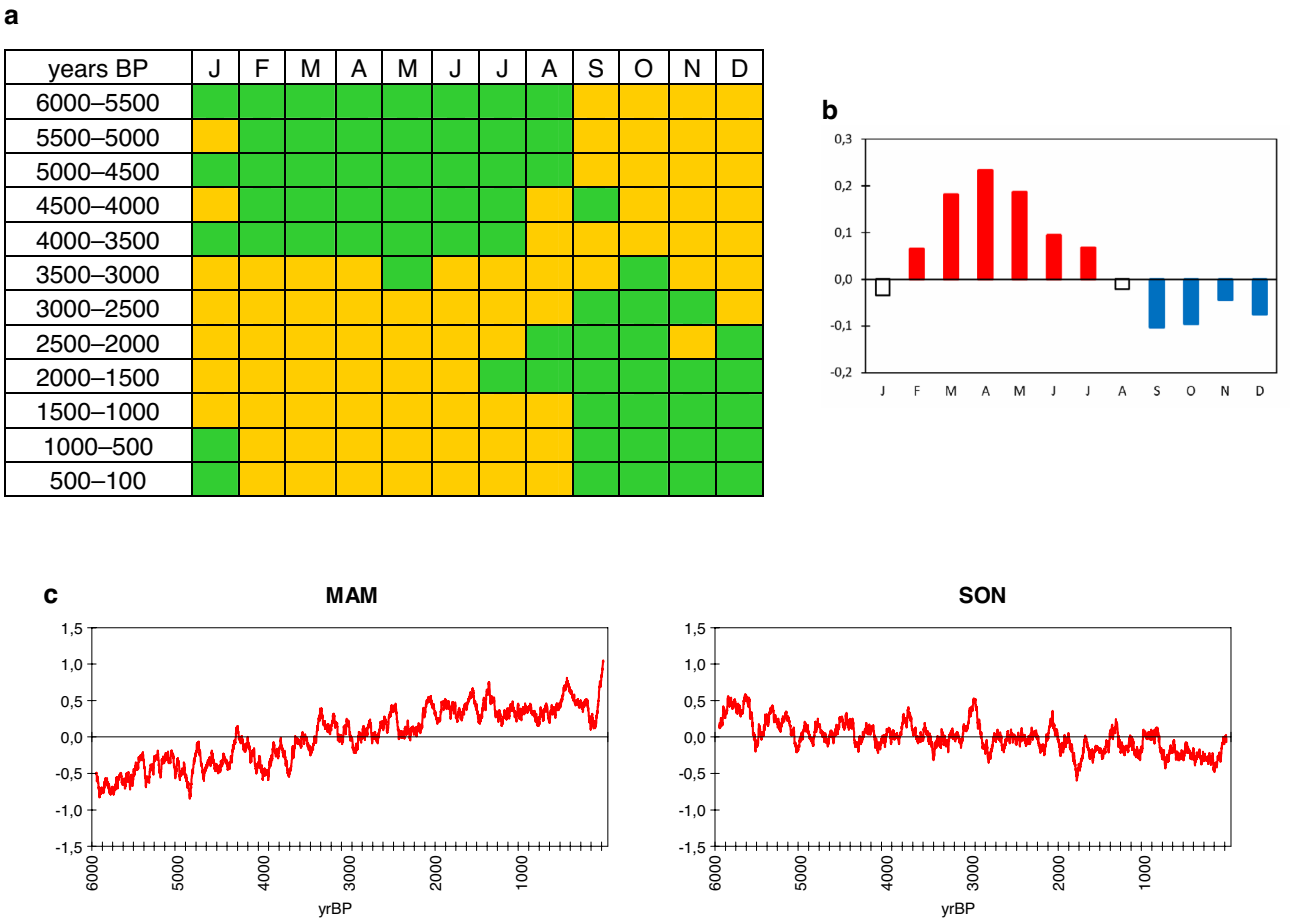

Fig. 3 **a** Sign of the SAM index simulated by the IPSL-CM5A2 model averaged over 500-year time windows. Positive (negative) values are indicated in orange (green). **b** Monthly linear trends of the SAM index on the whole period from 6000 years BP to 1849. Unit: 1/1000 year (the SAM index is dimensionless). Positive (negative) trends statistically significant at 99% according to the Student's *t* test are indicated in red (blue). **c** Seasonal time series of the SAM index in austral autumn (MAM) and spring (SON). Both time series are smoothed with a 100-year moving average

changes in extratropical meridional gradients summarize changes in the general structure of hemispheric SLP which can be described taking as a reference mean conditions and changes in austral autumn and spring. In autumn, zonal mean SLP decreases from 40° S to 65° S (Fig. 4c) but mean values increased in 40° S and decreased in 65° S from Mid- to Late-Holocene (Fig. 4c–e). Consequently, the meridional gradient increased through the study period (Fig. 4a, b). In spring, zonal mean SLP also decreases from 40° S to 65° S (Fig. 4d) but mean values decreased in 40° S and increased in 65° S from Mid- to Late-Holocene (Fig. 4d, e) weakening the meridional gradient (Fig. 4a, b).

Changes in atmospheric circulation described by the transient IPSL-CM5A2 model simulation can be compared with those of an ensemble mean of various paleoclimate simulations contained in the Paleoclimate Modeling Intercomparison Project Phase 3 (PMIP3; https://pmip3.lsce.ipsl.fr). In fact, PMIP3 simulations reconstruct the climate in ~ 6000 years BP and during the 1350–1850 period which are the time windows considered for MidH and LatH respectively. The comparison reveals that changes in SLP gradients described by the IPSL-CM5A2 model (Fig. 4a, b) are qualitatively similar to those of the ensemble mean of PMIP3 models (Supplementary Fig. S2a, b): the extratropical meridional gradient of SLP increased in austral autumn and decreased in spring while summer and winter are periods of transitions between them. Consequently, these modeled atmospheric circulation changes are coincident signals in the single IPSL-CM5A2 simulation and the average of various PMIP3 paleoclimate simulations. In other words, the single IPSL-CM5A2 simulation does not produce artificial signals of long-term atmospheric circulation change in the Southern Hemisphere.

Basic atmospheric dynamics concepts link the resulting changes in meridional pressure gradients to changes in near-surface temperature gradients between tropical and

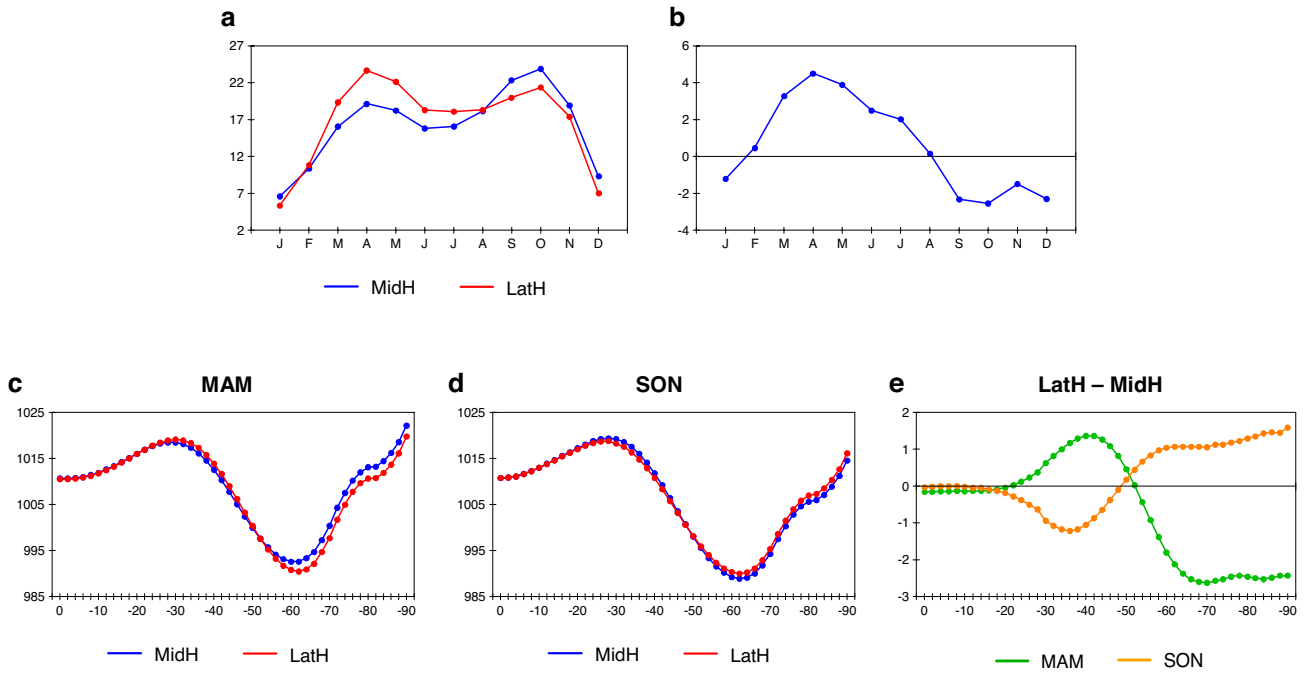

Fig. 4 **a** Meridional gradients of sea level pressure (SLP) in the Mid-Holocene (MidH) (blue) and Late Holocene (LatH) (red) calculated as differences of zonal means at 40° S minus zonal means at 65° S. Unit: hPa. **b** SLP gradients differences calculated as gradients in LatH minus gradients in MidH. **c** Autumn SLP zonal means in periods MidH (blue) and LatH (red). Unit: hPa. **d** Spring SLP zonal means in periods MidH (blue) and LatH (red). **e** SLP zonal mean differences calculated as zonal means in LatH minus zonal means in MidH

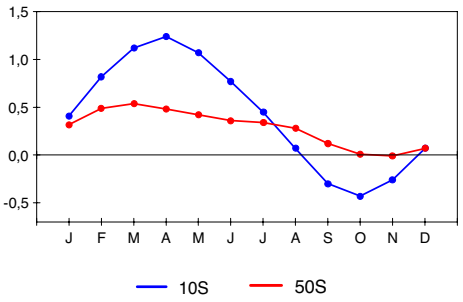

Fig. 5 Differences of temperature at 2 m (T2m) at 10° S (blue) and 50° S (red) calculated as T2m in the Late Holocene minus T2m in the Mid-Holocene. Unit: °C

extratropical regions in response to the slow changes in insolation from Mid- to Late-Holocene. In fact, the most intense warming over tropical-extratropical regions (i.e., the latitudinal band between 0° and 60° S) occurred in austral autumn (Fig. 5) being more pronounced at lower latitudes and, as a result, meridional temperature gradients intensified. Conversely, the most intense cooling over tropical-extratropical regions occurred in austral spring and meridional temperature gradients weakened due to more pronounced cooling at lower latitudes. As changes in SLP conditions, autumn and spring are the seasons when temperature changes are more pronounced while summer and winter are periods of transitions between them.

Temperature changes displayed in Fig. 5 indicate that the timing of the maximum (minimum) temperature anomaly is delayed by about one season relative to the beginning of insolation positive (negative) anomaly showed in Fig. 1. In fact, the increment (reduction) of insolation with respect to 6000 years BP conditions started in summer (winter) but the maximum warming (cooling) occurred during autumn (spring). Delayed response of the climate system to insolation changes was also found in previous model simulations analyzed by Renssen et al. (2005), Rojas and Moreno (2011), Renssen et al. (2012) and Varma et al. (2012). These studies suggested that the action of thermal inertia of the oceans and the influence of monsoon systems are factors that might have caused seasonal lags in the response of temperature to insolation changes. Regarding the influence of monsoon systems, increased summer insolation might reinforce monsoon systems creating moister conditions that reduce the surface heating and shift the maximum warming to autumn when the dry season starts. Concerning meridional conditions displayed in Fig. 5, values around zero during spring in ~ 50° S are a consequence of non-significant changes of temperature over subtropical oceans.

Considering that the SAM index synthesizes the strength of the meridional gradient of pressure anomalies

at middle and high Southern Hemisphere latitudes, SAM trends displayed in Fig. 3 imply long-term changes in position and/or intensity of westerly winds. In fact, there is a pronounced poleward shift of the latitude of maximum wind speed in austral autumn (Fig. 6a) that produce reinforced winds in the central and southern regions of the westerlies belt (i.e., the latitudinal band ~ 40° S–60° S) and weakened winds in the northern portion of the westerlies belt (Fig. 6c). In contrast, the latitude of maximum wind speed shifts toward the equator in spring (Fig. 6b) inducing weakened winds in the central and southern regions of the westerlies belt and reinforced winds to the north (Fig. 6c). Summer and winter constitute transitional states between the extreme inverse conditions developed in autumn and spring (figures not shown). These long-term changes in westerlies simulated by the IPSL-CM5A2 model are consistent with conclusions of previous model-based analyses developed by Varma et al. (2012) (analysis of Holocene transient simulations) and Rojas and Moreno (2011) and Berman et al. (2017) (analysis of differences between Mid-Holocene and pre-industrial time windows) indicating that they are robust signals in a wide variety of paleoclimatic model simulations. Furthermore, it is clear that the latitude of maximum wind speed shifted toward Antarctica when the SAM index increased from Mid- to Late-Holocene (i.e., months around autumn) while the westerlies tended to move toward the equator when the SAM index decreased (i.e., months around spring).

Results of the IPSL-CM5A2 transient simulation depicted in the previous paragraphs provide continued descriptions of long-term history of the climate system. Changes in temperature and intensity/position of southern westerlies in response to slow insolation changes from Mid- to Late-Holocene inferred from this simulation agree with results of previous model-based studies. In this context, our transient results bring into light novel information regarding long-term SAM variability allowing inferences of diverse monthly/seasonal behavior as well as different rate of changes.

4 Proxy-model comparisons

Validation of the 6000-year-long SAM index simulated by the IPSL-CM5A2 model against proxy-based records is a challenge due to the lack of reconstructions of the SAM covering more than the last millennium (see Sect. 1). The longer available reconstructions are those developed since AD 1000 by Abram et al. (2014) (hereafter referred as A14) for annual means and Dätwyler et al. (2018) (hereafter referred as D18) for annual and austral summer means (Fig. 7). Although these reconstructions do not allow to validate the SAM index in the entire 6000-year-long simulated period, proxy-model comparisons in the last millennium might bright into light useful information regarding model performance. In this context, it is important to mention that proxy-based SAM index are reconstructed considering information extracted from sites that are not geographically evenly distributed through middle and high Southern Hemisphere latitudes. Consequently, reconstructed index might have some deficiencies in representing zonal mean conditions involved in SAM variability. However, taking as reference the observational-based index of Marshall (2003), information extracted from few specific continental sites constitutes information highly representative of the circumpolar mean state of the SAM (Fogt and Marshall 2020). In other words, significant proxy-model disagreements should not be associated to the geographic distribution of sites which paleorecords were used to reconstruct long-term evolution of the SAM index.

The annual SAM index reconstructed by A14 (Fig. 7a) shows an initial period with not well-defined long-term trends until the end of ~ 1300 s when a pronounced negative trend or abrupt jump to lower values developed. Then, positive trend extended until ~ 1800s which is followed by negative trend until ~ 1940s and, finally, pronounced positive trend until the present. The general structure of these long-term changes agree reasonably well with the annual SAM index reconstructed by D18 (Fig. 7b) except by the

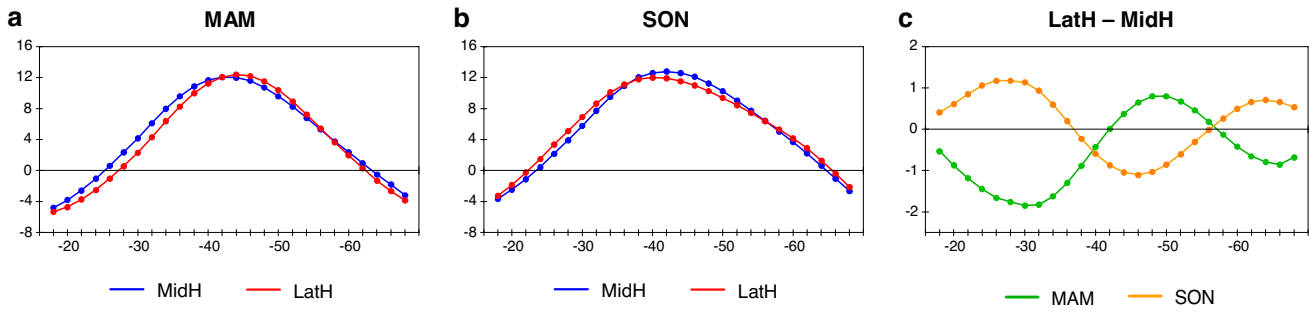

Fig. 6 **a** Autumn zonal means of the zonal component of wind at 850 hPa (U850) in the Mid-Holocene (MidH) (blue) and the Late Holocene (LatH) (red). Unit: m/s. **b** As **a** but for spring. **c** U850 zonal mean differences calculated as zonal means in LatH minus zonal means in MidH

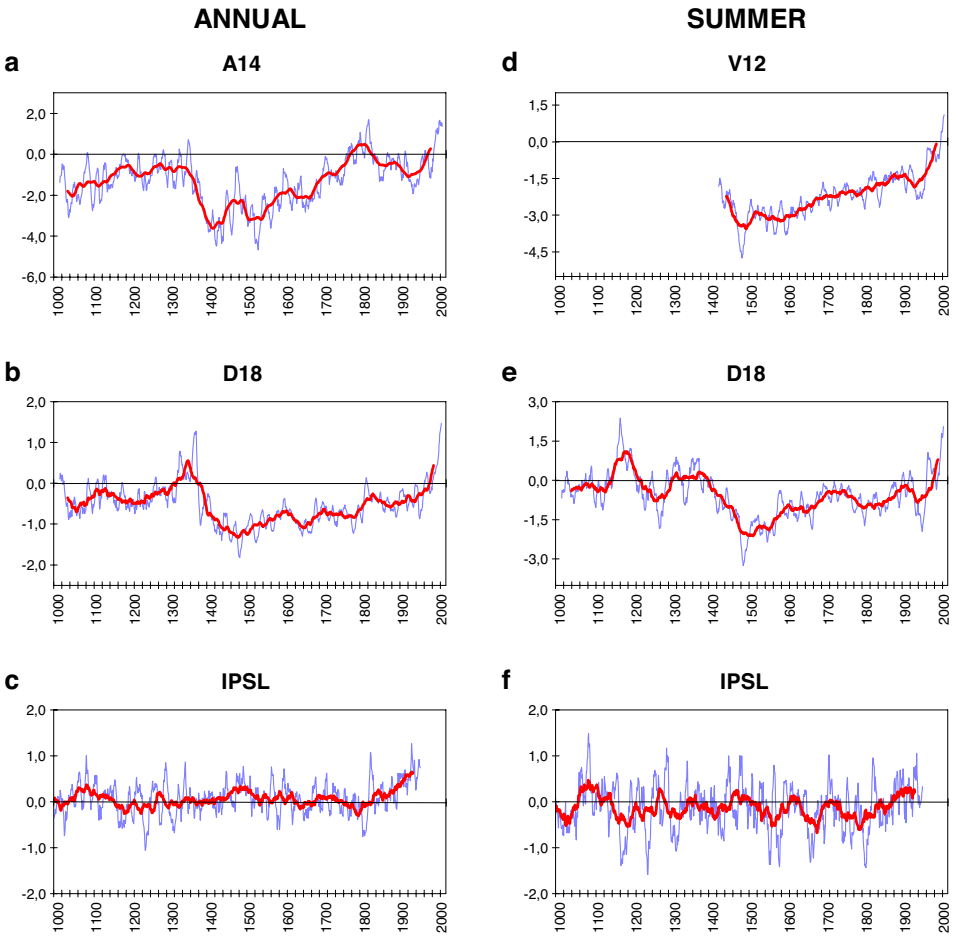

Fig. 7 Proxy-based and modeled SAM index for the past 1000 years. All indices are smoothed with a 10-year (blue) and 50-year (red) running mean. Proxy-based reconstructions correspond to Villalba et al. (2012) (V12), Abram et al. (2014) (A14), and Dätwyler et al. (2018) (D18). IPSL indicates the SAM index simulated by the IPSL-CM5A2 model

fact that the negative trend during 1800s and early 1900s suggested by A14 is not observed in D18 reconstruction (see also Supplementary Fig. S3a, b). Moreover, the summer SAM index reconstructed by D18 (Fig. 7e) shows a general structure similar to that reconstructed for annual means (Fig. 7b) that also agree well with the summer reconstruction developed by Villalba et al. (2012) (hereafter referred as V12) since AD 1409 (Fig. 7d).

Pronounced trends spanning past centuries, when the anthropogenic forcing was absent, inferred from paleo-records indicate that internal variability and/or natural forcings have influenced long-term SAM variability in the last millennium. Changes in solar irradiance and trends in tropical Pacific sea surface temperature (SST) have been proposed by A14 as possible forcings of SAM trends in pre-Industrial periods. Moreover, in the context of changes in the modern Industrial Era, the unusual positive trends observed in V12, A14 and D18 reconstructions since ~ 1950s were first described in reconstructions developed by Fogt et al. (2009) (hereafter referred as F09) (Supplementary Fig. S4).

Long-term time evolution of annual and summer SAM index simulated by the IPSL-CM5A2 model (Fig. 7c–f) differs from the available proxy-based reconstructions through the entire millennium. In fact, modeled SAM index show a lack of long-term trends until ~ 1800s when pronounced positive trends began. The lack of significant linear trends in modeled SAM index during the ~ 1000s–1800s period is observed in all months (figures not shown) and might be consequence of almost constant insolation forcing through that period in the model simulation (see Supplementary Fig. S1b).

Proxy-model disagreement in the time-window extended from ~ 1400s to ~ 1800s coincides with the period in which the Little Ice Age (LIA) developed. Consequently, the SAM behavior observed in proxy-based reconstructions might be associated to LIA climate forcings that are not properly reproduced by the IPSL-CM5A2 model simulation (e.g., volcanic activity, solar irradiance describing the Spörer Minimum in ~ 1500s and the Mounder Minimum in ~ 1700s). After this ~ 1400s–1800s period, and coinciding with the inclusion of anthropogenic forcing in the model simulation, a persistent positive trend starts in the modeled SAM index being an abrupt change not observed in proxy-based reconstructions (see Supplementary Fig. S3). Nevertheless, previous last millennium transient climate model simulations carried out as part of the Coupled Model Intercomparison

Project fifth phase (CMIP5) also show pronounced positive trend starting in ~ 1800s which was related to the fact that numerical models seem to be unable to reproduce climate conditions inferred from proxy data during the nineteenth century (Abram et al. 2014).

Limitations in model performance and/or uncertainties in the estimation of prescribed boundary conditions and forcings of climate variability in model simulations might produce the proxy-model disagreement detected in SAM reconstructions through the last millennium. However, alternative explanations may be related to limitations in proxy information. In fact, it is possible that the SAM was not the only forcing of climate variability through the last millennium in areas where the available proxy sites are located. Consequently, variability of proxy-based SAM reconstructions might contain information of other forcings affecting climate conditions in those areas that, in turn, affects the reconstruction of a "pure" SAM index. For instance, Southern Hemisphere areas affected by the SAM tend to be the same areas affected by the action of Rossby wave trains excited in the tropical Pacific (e.g., Mo 2000; Mo and Paegle 2001).

Whatever the reason of proxy-model disagreements detected in SAM reconstructions since ~ 1400s, those discrepancies should not affect the credibility of model-based results exposed in Sect. 3 because the main driver of climate changes in that 6000-year-long period was the orbital forcing that induced insolation changes displayed in Fig. 1.

5 Influence of Pacific Ocean SSTs on SAM long-term evolution

There are numerous evidences for influence of tropical Pacific SST on SAM variability during part of the last century (e.g., Fogt and Marshall 2020 and references therein). However, this relationship should be treated with caution due to the nonstationary nature of tropical-extratropical atmospheric connections in the Southern Hemisphere. Actually, Silvestri and Vera (2009) showed evidence that the significant link between tropical Pacific SSTs and the SAM index developed since the ~ 1980s was absent in previous decades of the twentieth century. Consequently, the close tropical-extratropical connection detected since the ~ 1980s should not be assumed as a persistent feature of Southern Hemisphere atmospheric circulation through the entire Holocene. High-quality and reliable proxy-based reconstructions are required to study that connection during past time windows. In this context, discrepancies among available reconstructions make it challenging to infer unambiguous signals of tropical Pacific SST evolution in the last millennium as well as its connection with SAM variability. Indeed, the positive trend in the A14 annual SAM index from the 16th to eighteenth century and the reversal of this trend during the nineteenth century (Supplementary Fig. S5a) might be mirror changes in the mean EN3.4 SST reconstructed by Emile-Geay et al. (2013) (Supplementary Fig. S5c) but that relationship is absent if the ENSO index reconstructed by Braganza et al. (2009) (Supplementary Fig. S5d) or the Interdecadal Pacific Oscillation (IPO) index reconstructed by Vance et al. (2015) (Supplementary Fig. S5e) and Porter et al. (2021) (Supplementary Fig. S5f) are considered. Furthermore, the persist positive trend since the sixteenth century in the D18 annual SAM index (Supplementary Fig. S5b) might be coincident with the long-term trend in the Porter's IPO index but disagree with the evolution of the Emile-Geay's EN3.4 index, Braganza's ENSO index, and Vance's IPO index. Moreover, the positive trends in the V12 and D18 summer SAM index since the fifteenth century (Supplementary Fig. S6a, b) disagree with the lack of long-term trends in the EN3.4 and EN3 indices reconstructed by Dätwyler et al. (2020), Li et al. (2013) and D'Arrigo et al. (2005) respectively (Supplementary Fig. S6c–e). In summary, available proxy-based reconstructions of Pacific SSTs make it difficult to have conclusive results regarding the influence of ocean conditions on long-term SAM changes through the last millennium.

In the context of Mid- to Late Holocene climate evolution simulated by the IPSL-CM5A2 model, the link between changes in meridional gradients of pressure and near-surface temperature described in Sect. 3 are coherent with simulated long-term changes in the IPO index. Actually, simulated Mid- to Late Holocene evolution of the IPO index is characterized by significant positive linear trends from summer to winter while significant negative trends developed in spring (Supplementary Table S3). As changes in meridional gradients of SLP and temperature, signs and magnitudes of seasonal linear trends indicate that the long-term evolution of the IPO index during autumn was inverse to that of spring while summer and winter were periods of transitions between them. In light of this result, long-term changes in the SAM might be forced by changes in the IPO index that, in turn, were influenced by the slow changes in insolation. However, to confirm this hypothesis and to assess the influence of the Pacific Ocean (including IPO conditions) on Mid- to Late Holocene evolution of the SAM, numerical experiments allowing SST changes only in the Pacific basin should be done with the IPSL-CM5A2 model. The SAM signal forced only by the Pacific should emerge from these experiments. Additionally, agreements among diverse proxy-based reconstructions of both Pacific SSTs (including the IPO index) and the SAM index are required in order to have reliable information to validate model simulations.

6 Conclusions

This study describes long-term changes of the SAM index from Mid- to Late Holocene based on the state-of-the-art transient simulation of the last 6000 years carried out with the IPSL-CM5A2 model. Due to the lack of proxy-based reconstructions, numerical model simulations constitute an essential tool to infer patterns of SAM evolution during this past period when changes in insolation in response to orbital forcing was the main driver of long-term changes in the climate system.

The modeled SAM index exhibits significant long-term linear trends, which sign reverses through the year. In fact, positive linear trends extend from February to July while negative trends develop from September to December. Slow changes in insolation and SAM are linked by physical mechanisms based on temperature and pressure changes developed over the Southern Hemisphere. Actually, model results indicate that insolation changes produced significant changes in meridional temperature gradients that, in turn, induced changes in meridional pressure gradients which are synthesized by changes in the SAM index.

Results exposed in this paper should be taken into account in proxy-based reconstructions of SAM index evolution through Middle and Late Holocene. One essential condition must be satisfied by the proxy network considered in those reconstructions: selected proxies must describe climate conditions at seasonal scale because model results show that the long-term SAM variability is not homogeneous through the year. Furthermore, paleorecords should not contain information of other patterns of atmospheric variability (as wave-trains excited in the tropical Pacific) that masked the "pure" SAM signal. Alternatively, congruent paleoclimatic reconstructions of westerlies wind behavior can help to infer a framework for past SAM evolution due to the close relationship between SAM and westerlies. However, this methodology is still problematic due to there are marked discrepancies between different proxy-based reconstructions of intensity and position of southern westerlies.

In summary, paleoclimate proxies and numerical model simulations constitute two essential and complementary tools to reconstruct past climate conditions. However, results exposed in this study indicate that both sources of information must be treated with caution when inferring SAM evolution in Mid- to Late Holocene. Actually, it is well known that reconstructed time-windows are restricted to the availability of paleorecords and all proxy-based climate reconstructions contain uncertainties inherent to the quality of used proxy records and the applied methodologies. Additionally, proxy records required to reconstruct the SAM might also be affected by other patterns of atmospheric circulation making difficult to detect and isolate time variability of the "pure" SAM index. On the other hand, the transient model simulation allows reconstructions of the "pure" SAM index at monthly time scale through the entire study period. This numerical simulation describes the impact of slow changes in insolation through Middle and Late Holocene which is the dominant long-term signal in modeled extratropical meridional gradients of pressure. Nevertheless, multidecadal variability of atmospheric circulation encompassed in the SAM index and associated to the influence of individual oceanic basins might be captured more accurately by discrete proxy data affected by those regional SSTs. Consequently, to have a suitable and reliable proxy-based reconstruction of SAM index evolution through Middle and Late Holocene is highly valuable to validate transient paleoclimatic model simulations which provide an historical context for both present-day variability and projected future changes of the climate system in response to anthropogenic forcings.

Supplementary Information The online version contains supplementary material available at https://doi.org/10.1007/s00382-022-06160-0.

Acknowledgements The authors appreciate comments and suggestions provided by Dr. Chris Brierley and an anonymous reviewer which were very helpful in improving this paper. Pascale Braconnot and Olivier Marti acknowledge PRACE for awarding them access to Curie at GENCI@CEA, France (THROL project). The transient simulation was also performed using HPC resources from GENCI-TGCC thanks to a high-end computing access grant and annual LSCE allocation time (gen2212). Model developments and infrastructure is supported by the IPSL Modeling Center and benefits from the L-IPSL LABEX and IPSL Climate Graduate School (Investissements d'avenir programme ANR-11-IDEX-0004-17-EURE-0006).

Author contributions All authors contributed to the study conception and design. The first draft of the manuscript was written by GS and all authors commented on previous versions of the manuscript. All authors read and approved the final manuscript.

Funding Model developments and infrastructure is supported by the IPSL Modeling Center and benefits from the L-IPSL LABEX and IPSL Climate Graduate School (Investissements d'avenir programme ANR-11-IDEX-0004-17-EURE-0006).

Data availability The datasets generated during and/or analyzed during the current study are available from the authors on reasonable request.

Declarations

Conflict of interest The authors have no relevant financial or non-financial interests to disclose.

References

Abram N, Mulvaney R, Vimeux F et al (2014) Evolution of the Southern Annular Mode during the past millennium. Nat Clim Change 4(7):564–569

Arblaster JM, Meehl GA (2006) Contributions of external forcings to southern annular mode trends. J Clim 19(12):2896–2905

Baldwin MP (2001) Annular modes in global daily surface pressure. Geophys Res Lett 28(21):4115–4118

Berman AL, Silvestri G, Rojas M, Tonello M (2017) Accelerated greenhouse gases versus slow insolation forcing induced climate changes in southern South America since the Mid-Holocene. Clim Dyn 48:387–404

Braconnot P, Crétat J, Marti O, Balkanski Y, Caubel A, Cozic A, Foujols M-A, Sanogo S (2019) Impact of multiscale variability on last 6,000 years Indian and West African monsoon rain. Geophys Res Lett 46(23):14021–14029

Braganza K, Gergis JL, Power SB, Risbey JS, Fowler AM (2009) A multiproxy index of the El Niño-Southern Oscillation, A.D. 1525–1982. J Geophys Res 114:D05106. https://doi.org/10.1029/2008JD010896

Cai W, Watterson IG (2002) Modes of interannual variability of the Southern Hemisphere circulation simulated by the CSIRO climate model. J Clim 15(10):1159–1174

Cai W, Whetton PH, Karoly DJ (2003) The response of the Antarctic Oscillation to increasing and stabilized atmospheric CO2. J Clim 16(10):1525–1538

Crétat J, Braconnot P, Terray P, Marti O, Falasca F (2020) Mid-Holocene to present-day evolution of the Indian monsoon in transient global simulations. Clim Dyn 55:2761–2784

D'Arrigo R, Cook ER, Wilson RJ, Allan R, Mann ME (2005) On the variability of ENSO over the past six centuries. Geophys Res Lett 32:L03711. https://doi.org/10.1029/2004GL022055

Dätwyler C, Neukom R, Abram NJ, Gallant AJE, Grosjean M, Jacques-Coper M, Karoly DJ, Villalba R (2018) Teleconnection stationarity, variability and trends of the Southern Annular Mode (SAM) during the last millennium. Clim Dyn 51:2321–2339

Dätwyler C, Grosjean M, Steiger NJ, Neukom R (2020) Teleconnections and relationship between the El Niño-Southern Oscillation (ENSO) and the Southern Annular Mode (SAM) in reconstructions and models over the past millennium. Clim past 16:743–756

Dufresne J-L, Foujols M-A, Denvil S et al (2013) Climate change projections using the IPSL-CM5 Earth System Model: from CMIP3 to CMIP5. Clim Dyn 40(9–10):2123–2165

Emile-Geay J, Cobb K, Mann M, Wittenberg A (2013) Estimating central equatorial Pacific SST variability over the past millennium. Part II: reconstructions and implications. J Clim 26:2329–2352

Fogt RL, Bromwich DH (2006) Decadal variability of the ENSO teleconnection to the high-latitude South Pacific governed by coupling with the southern annular mode. J Clim 19(6):979–997

Fogt RL, Marshall GJ (2020) The Southern Annular Mode: variability, trends, and climate impacts across the Southern Hemisphere. Wires Clim Change 11:e652. https://doi.org/10.1002/wcc.652

Fogt RL, Perlwitz J, Monaghan AJ, Bromwich DH, Jones JM, Marshall GJ (2009) Historical SAM variability. Part II: twentieth-century variability and trends from reconstructions, observations, and the IPCC AR4 models. J Clim 22(20):5346–5365

Fogt RL, Goergens CA, Jones JM, Schneider DP, Nicolas JP, Bromwich DH, Dusselier HE (2017) A twentieth century perspective on summer Antarctic pressure change and variability and contributions from tropical SSTs and ozone depletion. Geophys Res Lett 44(19):9918–9927

Gillett NP, Thompson DWJ (2003) Simulation of recent Southern Hemisphere climate change. Science 302(5643):273–275

Gong D, Wang S (1999) Definition of Antarctic oscillation index. Geophys Res Lett 26(4):459–462

Hernández A, Martin-Puertas C, Moffa-Sánchez P et al (2020) Modes of climate variability: Synthesis and review of proxy-based reconstructions through the Holocene. Earth Sci Rev 209:103286. https://doi.org/10.1016/j.earscirev.2020.103286

Hessl A, Allen K, Vance T, Abram N, Saunders K (2017) Reconstructions of the southern annular mode (SAM) during the last millennium. Prog Phys Geogr 41(6):834–849

Huiskamp W, McGregor S (2020) Quantifying paleo-reconstruction skill of the Southern Annular Mode in a model framework. Clim Past Discuss. https://doi.org/10.5194/cp-2020-133

Jones JM, Widmann M (2003) Instrument- and tree-ring-based estimates of the Antarctic Oscillation. J Clim 16:3511–3524

Kageyama M, Braconnot P, Bopp L et al (2013a) Mid-Holocene and Last Glacial Maximum climate simulations with the IPSL model—Part I: comparing IPSL_CM5A to IPSL_CM4. Clim Dyn 40:2447–2468

Kageyama M, Braconnot P, Bopp L et al (2013b) Mid-Holocene and last glacial maximum climate simulations with the IPSL model: part II: model-data comparisons. Clim Dyn 40:2469–2495

Kageyama M, Braconnot P, Harrison SP, Haywood AM, Jungclaus JH, Otto-Bliesner BL et al (2018) The PMIP4 contribution to CMIP6—part 1: overview and over-arching analysis plan. Geosci Model Dev 11(3):1033–1057

Kidson JW (1988) Interannual variations in the Southern Hemisphere circulation. J Clim 1:1177–1198

Kidson JW (1999) Principal modes of Southern Hemisphere low-frequency variability obtained from NCEP–NCAR Reanalyses. J Clim 12(9):2808–2830

Kuroda Y, Kodera K (2005) Solar cycle modulation of the Southern Annular Mode. Geophys Res Lett 32:L13802. https://doi.org/10.1029/2005GL022516

Kuroda Y, Shibata K (2006) Simulation of solar-cycle modulation of the Southern Annular Mode using a chemistry-climate model. Geophys Res Lett 33:L05703. https://doi.org/10.1029/2005GL025095

Laprida C, Orgeira MJ, Fernández M, Tófalo R, Ramón Mercau J, Silvestri G, Berman AL, García Chapori N, Plastani MS, Alonso S (2021) The role of Southern Hemispheric Westerlies for Holocene hydroclimatic changes in the steppe of Tierra del Fuego (Argentina). Quatern Int 571:11–25

Li J, Xie SP, Cook E et al (2013) El Niño modulations over the past seven centuries. Nat Clim Change 3:822–826. https://doi.org/10.1038/nclimate1936

Limpasuvan V, Hartmann DL (2000) Wave-maintained annular modes of climate variability. J Clim 13:4414–4429

Marshall G (2003) Trends in the Southern Annular Mode from observations and reanalyses. J Clim 16:4134–4143

Mignot J, Bony S (2013) Presentation and analysis of the IPSL and CNRM climate models used in CMIP5. Clim Dyn 40(9–10):2089–2089

Miller RL, Schmidt GA, Shindell DT (2006) Forced annular variations in the 20th century intergovernmental panel on climate change fourth assessment report models. J Geophys Res 111(D18). https://doi.org/10.1029/2005JD006323

Mo KC (2000) Relationships between low-frequency variability in the Southern Hemisphere and sea surface temperature anomalies. J Clim 13:3599–3610

Mo KC, Paegle JN (2001) The Pacific-South American modes and their downstream effects. Int J Climatol 21:1211–1229

Polvani LM, Waugh DW, Correa GJP, Son S-W (2011) Stratospheric ozone depletion: the main driver of twentieth-century atmospheric circulation changes in the Southern Hemisphere. J Clim 24(3):795–812

Porter SE, Mosley-Thompson E, Thompson LG, Wilson AB (2021) Reconstructing an Interdecadal Pacific Oscillation Index from a Pacific basin–wide collection of ice core records. J Clim 34:3839–3852

Renssen H, Goosse H, Fichefet T, Masson-Delmotte V, Koç N (2005) Holocene climate evolution in the high-latitude Southern Hemisphere simulated by a coupled atmosphere-sea ice-ocean-vegetation model. Holocene 15(7):951–964

Renssen H, Seppa H, Crosta X, Goosse H, Roche DM (2012) Global characterization of the Holocene Thermal Maximum. Quat Sci Rev 48:7–19

Rogers JC, van Loon H (1982) Spatial variability of sea level pressure and 500 mb height anomalies over the Southern Hemisphere. Mon Weather Rev 110(10):1375–1392

Rojas M, Moreno PI (2011) Atmospheric circulation changes and neoglacial conditions in the Southern Hemisphere mid-latitudes: insights from PMIP2 simulations at 6 kyr. Clim Dyn 37:357–375

Sepulchre P, Caubel A, Ladant J-B et al (2020) IPSL-CM5A2—an Earth System Model designed for multi-millennial climate simulations. Geosci Model Dev 13:3011–3053

Sexton DMH (2001) The effect of stratospheric ozone depletion on the phase of the Antarctic Oscillation. Geophys Res Lett 28:3697–3700

Shindell DT, Schmidt G (2004) Southern Hemisphere climate response to ozone changes and greenhouse gas increases. Geophys Res Lett 31(18). https://doi.org/10.1029/2004GL020724

Silvestri G, Vera C (2009) Nonstationary impacts of the Southern Annular Mode on Southern Hemisphere climate. J Clim 22:6142–6148

Thompson DWJ, Solomon S (2002) Interpretation of recent Southern Hemisphere climate change. Science 296(5569):895–899

Thompson DWJ, Wallace J (2000) Annular modes in the extratropical circulation. Part I: month-to-month variability. J Clim 13:1000–1016

Thompson DWJ, Solomon S, Kushner P et al (2011) Signatures of the Antarctic ozone hole in Southern Hemisphere surface climate change. Nat Geosci 4:741–749. https://doi.org/10.1038/ngeo1296

Vance TR, Roberts JL, Plummer CT, Kiem AS, van Ommen TD (2015) Interdecadal Pacific variability and eastern Australian megadroughts over the last millennium. Geophys Res Lett 42:129–137. https://doi.org/10.1002/2014GL062447

Varma V, Prange M, Merkel U, Kleinen T, Lohmann G, Pfeiffer M, Renssen H, Wagner A, Wagner S, Schulz M (2012) Holocene evolution of the Southern Hemisphere westerly winds in transient simulations with global climate models. Clim past 8:391–402

Villalba R, Lara A, Masiokas MH, Urrutia R, Luckman BH, Marshall GJ, Mundo IA, Christie DA, Cook ER, Neukom R et al (2012) Unusual Southern Hemisphere tree growth patterns induced by changes in the Southern Annular Mode. Nat Geosci 5:793–798

Visbeck M (2009) A station-based Southern Annular Mode index from 1884 to 2005. J Clim 22(4):940–950

Wilks DS (2006) Statistical methods in the atmospheric sciences, 2nd edn. International Geophysics Series. Elsevier Academic Press, St. Louis

Zhang Z-Y, Dao-Yi G, Xue-Zhao H, Yang-Na L, Sheng-Hui F (2010) Statistical reconstruction of the Antarctic Oscillation index based on multiple proxies. Atmos Ocean Sci Lett 3(5):283–287